THE JOURNAL OF BIOLOGICAL CHEMISTRY
Vol. 277, No. 47, Issue of November 22, pp. 44722–44730, 2002
Printed in U.S.A.

Homer Regulates Gain of Ryanodine Receptor Type 1 Channel Complex*

Received for publication, July 30, 2002, and in revised form, August 27, 2002
Published, JBC Papers in Press, September 9, 2002, DOI 10.1074/jbc.M207675200

Wei Feng‡, Jiancheng Tu§, Tianzhong Yang¶, Patty Shih Vernon§, Paul D. Allen¶, Paul F. Worley§, and Isaac N. Pessah‡‖

From the ‡Department of Molecular Biosciences, University of California, Davis, California 95616, the §Department of Neuroscience, The Johns Hopkins University School of Medicine, Baltimore, Maryland 21205, and the ¶Department of Anesthesia, Preoperative and Pain Medicine, Brigham and Women's Hospital, Boston, Massachusetts 02115

Homer proteins form an adapter system that regulates coupling of group 1 metabotropic glutamate receptors with intracellular inositol trisphosphate receptors and is modified by neuronal activity. Here, we demonstrate that Homer proteins also physically associate with ryanodine receptors type 1 (RyR1) and regulate gating responses to Ca^{2+}, depolarization, and caffeine. In contrast to the prevailing notion of Homer function, Homer1c (long form) and Homer1-EVH1 (short form) evoke similar changes in RyR activity. The EVH1 domain mediates these actions of Homer and is selectively blocked by a peptide that mimics the Homer ligand. 1B5 dyspedic myotubes expressing RyR1 with a point mutation of a putative Homer-binding domain exhibit significantly reduced (~33%) amplitude in their responses to K^+ depolarization compared with cells expressing wild type protein. These results reveal that in addition to its known role as an adapter protein, Homer is a direct modulator of Ca^{2+} release gain. Homer is the first example of an "adapter" that also modifies signaling properties of its target protein. The present work reveals a novel mechanism by which Homer directly modulates the function of its target protein RyR1 and excitation-contraction coupling in skeletal myotubes. This form of regulation may be important in other cell types that express Homer and RyR1.

Homer proteins are adapters that physically bind and functionally couple target proteins (1, 2). Homer1, Homer2, and Homer3 are encoded by three mammalian genes whose expression is dynamically regulated by cellular activity (2) and can attain high levels of protein in the nervous system where their functional regulation of excitatory signaling has been studied (3–5). A common element of structure of all Homer proteins is an N-terminal Enabled/Vasp homology domain (EVH1) essential for binding Homer ligands (6–7). Crystallographic analysis of the EVH1 domain binding surface has revealed its specific association with polyproline ligands (7) that have previously been defined within plasmalemmal glutamate receptors including mGluR1a[1] and mGluR5a/b (1), inositol 1,4,5-trisphosphate receptors (IP_3R) localized within endoplasmic and sarcoplasmic reticulum (SR) membranes (1), and cytoplasmic Shank proteins that are part of the N-methyl-D-aspartate receptor-associated PSD-95 complex (8, 9). A C-terminal coiled-coil domain is responsible for Homer self-multimerization (10–13). Although full-length Homer proteins are constitutively expressed in a number of tissues, immediate-early gene products of the Homer1 gene including Homer1a and Ania 3 lack the CC domain (3, 10). "Short form" Homer1a is rapidly and transiently induced by physiological synaptic stimuli that evoke long term potentiation in the hippocampus (3, 10) or *in striatum* by the addition of dopaminergic drugs (3). Thus, a use-dependent exchange of multimeric and protomeric short forms of Homer appears to be responsible for dynamic regulation of context-dependent signaling in neurons.

The functional influences of Homer adaptors on targeted protein have not been identified. Multi-PDZ domain proteins have been reported to cluster membrane ion channels with the result that the channel become active, but this effect is mimicked by agents that otherwise cross-link the channel (14). Homer binding to mGluR1 was recently reported to define agonist-independent activity of the receptor (15); however, this report did not define a molecular mechanism. The direct consequence of forming Homer-IP_3R complexes on the dynamics of endoplasmic reticulum/SR Ca^{2+} release and its possible contribution to temporal and spatial aspects of Ca^{2+} signals remain unclear.

Recently all three Homer mRNAs have also been detected in striated muscle, and Homer protein has been identified within skeletal and cardiac muscle (4, 5). Moreover, putative Homer ligand sequences are found within both the type 1 ryanodine receptor (RyR1) and the α_{1S}-subunit of the dihydropyridine receptor (DHPR; CACNA1S) of skeletal muscle (7). RyR1 assembles as tetrameric structures within junctional regions of SR where it forms large organized arrays (16). RyR1 forms physical associations with α_{1S}-DHPR that are essential for engaging reciprocal signaling units that are essential for excitation-contraction (E-C) coupling, a process whereby depolarization in the T-tubules triggers Ca^{2+} release from SR resulting in muscle contraction (17). Although Homer ligand consensus sequences reside in RyR1, experimental evidence confirming the physical association of Homer protein with RyR1, its functional influence on channel gating, and its pos-

* This work was supported by National Institutes of Health Grants AR17605 (to P. D. A. and I. N. P.), ES10173 and ES11269 (to I. N. P.), and DA10309 and MH01153 (to P. F. W.). The costs of publication of this article were defrayed in part by the payment of page charges. This article must therefore be hereby marked "*advertisement*" in accordance with 18 U.S.C. Section 1734 solely to indicate this fact.

‖ To whom correspondence should be addressed: Dept. of Molecular Biosciences, School of Veterinary Medicine, One Shields Ave., University of California, Davis, CA 95616. E-mail: inpessah@ucdavis.edu.

[1] The abbreviations used are: mGluR, group 1 metabotropic glutamate receptor; IP_3R, inositol 1,4,5-trisphosphate receptor(s); SR, sarcoplasmic reticulum; Ry, ryanodine; RyR1, type 1 ryanodine receptor; DHPR, dihydropyridine receptor; E-C, excitation-contraction; GST, glutathione *S*-transferase; PBS, phosphate-buffered saline; MOPS, 4-morpholinepropanesulfonic acid; CHAPS, 3-[(3-cholamidopropyl)dimethylammonio]-1-propanesulfonic acid; BLM, bilayer lipid membrane; CICR, Ca^{2+}-induced Ca^{2+} release; HLM, Homer ligand mutation.

sible physiological involvement in regulating E-C coupling are lacking. The presence of putative Homer ligand sequences on both RyR1 and α_{1S}-DHPR within skeletal myotubes provides an excellent system not only to understand the determinants underlying the interaction of Homer proteins with RyR but also to define their functional and physiological significance. The present paper shows that the direct physical interaction of Homer proteins with RyR1 results in a potent (nanomolar) amplification of channel responses to physiological and pharmacological signals. Homer-RyR1 complexes described here regulate the gain associated with E-C coupling and may likely have broad significance in physical and functional coupling of Ca^{2+} release units in excitable cells.

MATERIALS AND METHODS

Preparation of SR Membranes—Junctional SR membrane vesicles enriched in RyR1 were prepared from skeletal muscle of New Zealand White rabbits according to the method of Saito *et al.* (18) with some modifications (19). The preparations were stored in 10% sucrose, 10 mM HEPES, pH 7.4, at −80 °C until needed. Functional experiments reported were performed on four different SR preparations.

Expression and Purification of Homer Construct—GST fusion constructs were made by PCR amplifying the H1c open reading frame and the N-terminal 360-bp fragment with in frame primers with *Sal*I and *Not*I sites and inserting the PCR products into pGEX4T-2 (Pharmacia Corp.). Homer1-EVH1 W24A mutant was made with the QuikChange™ site-directed mutagenesis kit (Stratagene). Mena EVH1 GST was a gift from Dr. Leahy (Johns Hopkins and Howard Hughes Medical Institute). GST fusion plasmids of H1c, Homer1-EVH1 W24A, and Mena were transformed into BL21 cells, and positive clones were expanded. The cells were lysed by sonication, and the lysate was added to 1 ml of glutathione-agarose (Sigma) and sequentially washed as described previously (8, 9). A slurry of glutathione-agarose beads loaded with fusion protein was incubated with 5 units of biotinylated thrombin (Novagen). Purified Homer proteins were dialyzed against phosphate-buffered saline (PBS) at 4 °C overnight.

Construction and Expression of Putative Homer-binding Mutations in RyR1 cDNA—A 0.5-kb fragment was isolated between nucleotide 5064 (*Pml* site) and nucleotide 5582 (*Bgl*II site), and one 0.9-kb fragment (between nucleotide 14312, *Cla*I site and 15230, *Xba*I site) was isolated from the full-length RyR1 cDNA in pHSV/RyR1 to make the F1777R and F1782R mutations, respectively. The fragments were cloned in pBluescript-SK(+), and a QuikChange™ site-directed mutagenesis kit (Stratagene) was used to introduce F1777R/F1782R into the fragments. After confirming their sequence, the mutated fragments were cloned into the full-length RyR1. Wild type and mutated cDNAs were packaged in HSV-1 amplicon virions and expressed in 1B5 (RyR null) myotubes as previously described (21).

Homer-binding Peptides—Peptide mGluR5WT, $Pept_{wt}$ (ALTPPSPFRD), and mutant, $Pept_{mut}$ (ALTPPSPRRD) were synthesized on a PE Biosystems 430A peptide synthesizer using *N*-(9-fluorenyl)methoxycarbonyl (Fmoc) chemistry, purified by reverse-phase high pressure liquid chromatography, and analyzed by mass spectrometry.

Co-immunoprecipitation and GST Pull-down of Homer-RyR1 Complex—Rat skeletal muscle was homogenized and sonicated in 20 volumes of ice-cold 10 mM MOPS buffer containing 1% CHAPS with protease inhibitors and centrifuged for 10 min at 100,000 × *g* 4 °C. Three microliters of anti-Homer immune serum (8) or preimmune serum was added to 60 μl of tissue extract and incubated overnight at 4 °C. 50 μl of protein A-Sepharose slurry was washed, added to the antibody-extract mixture, and incubated for an additional 2 h. The beads were washed three times with ice-cold MOPS/CHAPS. Bound protein was eluted with 4% SDS loading buffer and analyzed by SDS-PAGE and Western blot. For pull-down assays skeletal muscle detergent extracts were prepared as described for co-immunoprecipitation and mixed with glutathione beads loaded with GST or GST-Homer proteins, incubated overnight, and washed three times with ice-cold MOPS/CHAPS.

Immunocytochemical and Western Blot Analyses of Homer and RyR Proteins—Differentiated 1B5 myotubes were fixed in cold (−20 °C) methanol and washed with PBS (Invitrogen). The cells were then permeabilized before blocking with PBS with 5% normal goat serum. Either anti-RyR1 34C monoclonal antibody (Developmental Studies Hybridoma Bank, University of Iowa, Iowa City, IA) (22) or anti-Homer1 polyclonal were applied at concentrations of 1:25 and 1:10, respectively. The cells were washed with PBS with 5% normal goat serum before incubated with Cy-3-conjugated goat anti-mouse IgG or goat anti-rabbit (1:1000) (Jackson ImmunoResearch Laboratories, Inc., West Grove, PA). Cy-3 fluorescence was visualized using a Nikon Diaphot microscope (Nikon, Melville, NY) with an epifluorescence attachment (excitation, 510–560 nm; emission, 590 nm).

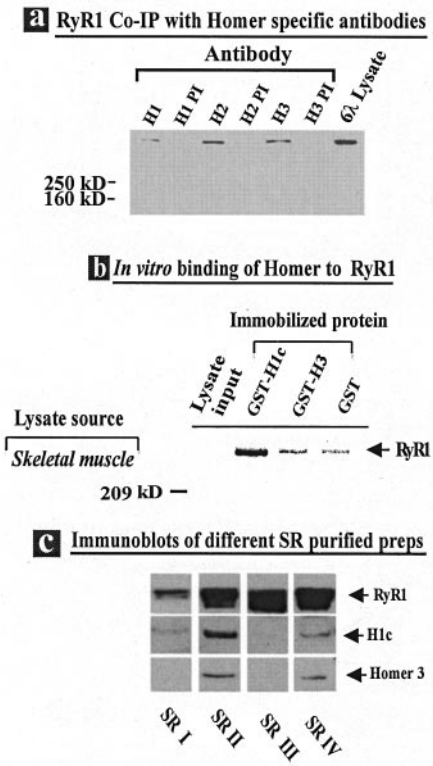

FIG. 1. **Physical association of homer with RyR.** The physical interactions between RyR1 and Homer proteins were analyzed by co-immunoprecipitation (*a*), GST-pull-down assays (*b*), and Western analysis of purified junctional SR membranes (*c*). In *a*, extracts of skeletal muscle SR in 1% CHAPS buffer were incubated with Homer antibodies (Homer1c, Homer2, and Homer3). The immunoprecipitates were probed with anti-RyR antibody 34C (22). Control lanes (*lanes* denoted as *H1 PI*, *H2 PI*, and *H3 PI*) utilized the preimmune serum of each antibody. The last lane (*6λ Lysate*) was the offered sample. In *b*, pull-down assays with GST-Homer fusion proteins and detergent extracts of skeletal muscle enriched in RyR1 were performed. RyR1 bound Homer1c and Homer3 GST proteins, whereas they did not bind to GST alone. In *c*, junctional SR membranes from four rabbits were separately prepared (preparations (*preps*) I–IV) and probed for RyR1 and Homer proteins by Western blot analysis. Junctional SR (30 μg of protein from each preparation) was applied onto SDS-PAGE, transferred to polyvinylidene difluoride membrane, and probed by anti-RyR1, Homer1c, and Homer3 antibodies.

Gel electrophoresis and Western blot analysis were described in detail elsewhere (23). Denatured protein (0.5–20 μg) was loaded onto 5% SDS-PAGE gels, electrophoresed, and then transferred onto polyvinylidene difluoride membranes. The blots were probed with 34C (1:200 dilution) or anti-H1 polyclonal (1:100). The immunoblots were rinsed and then incubated either with a horseradish peroxidase-conjugated sheep anti-mouse IgG 1:20,000 (for blots probed with 34C) or goat anti-rabbit IgG 1:10,000 (for blots probed with anti-H1; Sigma). Enhanced chemiluminescence techniques (PerkinElmer Life Sciences) were used to visualize the immunoblots.

Measurement of [^{3}H]Ryanodine Binding—Equilibrium measurement of specific high affinity [^{3}H]ryanodine ([^{3}H]Ry) binding was determined according to the method of Pessah *et al.* (24–26). SR vesicles (50 μg protein/ml) were incubated with or without Homer protein (50 nM) in assay buffer containing 20 mM HEPES, pH 7.1, 250 mM KCl, 15 mM NaCl, 100 nM to 10 μM $CaCl_2$, and 0.5 nM or 5 nM [^{3}H]Ry for 3 h at 37 °C. Complete saturation binding curves were performed using the "cold titration" method (24). The reactions were quenched by filtration through GF/B glass fiber filters and washed twice with ice-cold harvest buffer (20 mM Tris-HCl, 250 mM KCl, 15 mM NaCl, 50 μM $CaCl_2$, pH 7.1). Nonspecific binding was determined by incubating SR vesicles with 1000-fold excess unlabelled ryanodine.

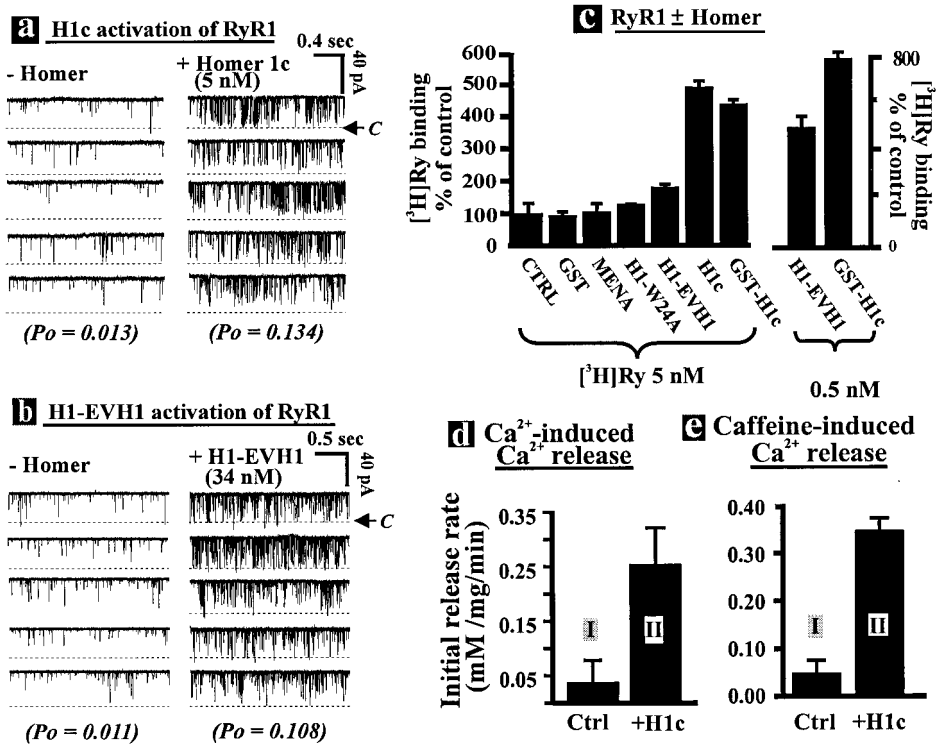

FIG. 2. **Functional modulation of RyR1 by Homer.** *a* and *b* show representative current traces of RyR1 channel activity in BLM before and after introduction of exogenous H1c (*a*) or H1-EVH1 (*b*) into the *cis* side of the channel. The current fluctuation through each channel was recorded at −40 mV. Cytosolic [Ca^{2+}] was 7 μM. The open probability (P_o) of the channel before and after exposed to the indicated concentration of Homer was averaged from a 2–5-min recording and denoted in the figure. The *dashed lines* indicate the open channel state, and the closed state (zero current) is indicated by the *arrows* (←*C*). The experiments were repeated with different single channels on separated BLM yielding similar results (*a*, $n = 4$; *b*, $n = 3$). *c* revealed that the binding of 5 nM (saturating) or 0.5 nM [^{3}H]Ry to 50 μg/ml of junctional SR-bound RyR1 in the presence of 350 nM free Ca^{2+} was unaffected by control medium (*CTRL*), 50 nM GST fusion protein (*GST*), or a murine Ena homolog, Mena EVH1 (*MENA*). Either 50 nM Homer1c (*H1c*) or 50 nM Homer1c-GST (*GST-H1c*) enhanced occupancy >5-fold, whereas the Homer1 EVH1 (*H1-EVH1*) was less active (<2-fold enhancement, $p < 0.05$) when tested at saturating at 5 nM [^{3}H]ryanodine. The H1-EVH1 point mutant at 50 nM (*H1-W24A*) lacked significant RyR1 activity. The data shown are the means ± S.E. from at least four replicates. The maximum efficacy of 50 nM GST-H1c was ~8-fold, and that of 150 nM H1-EVH1 was ~5-fold when tested at 0.5 nM [^{3}H]ryanodine (a concentration of ryanodine below its K_D) showing that H1a-EVH1 is 3-fold less potent than H1c for enhancing [^{3}H]ryanodine binding. *d* and *e* show that Homer enhances responsiveness of RyR1 to Ca^{2+} and caffeine, respectively. SR vesicles (50 μg/ml) were incubated as described under "Materials and Methods" for measuring macroscopic Ca^{2+} fluxes. After 160 μM Ca^{2+} was actively loaded into SR vesicles, 8 nM H1c (*II*) or the same volume of PBS (*I*) was introduced. After about 5 min, 80 μM Ca^{2+} (*d*; Ca^{2+}-induced Ca^{2+} release) or 10 mM caffeine (*e*; caffeine-induced Ca^{2+} release) was added to initiate release of Ca^{2+} accumulated during the loading phase. The initial Ca^{2+} release rates in the presence (*II*) or absence (*I*) of H1c were analyzed and plotted. The initial rate of Ca^{2+}-induced Ca^{2+} release increased from 0.002 ± 0.03 to 0.337 ± 0.029 μmol mg^{-1} min^{-1} in the presence of H1c ($n = 16$). Caffeine-induced Ca^{2+} release increased from 0.009 ± 0.045 to 0.249 ± 0.076 μmol mg^{-1} min^{-1} in the presence of H1c ($n = 11$).

Single Channel Kinetics in Bilayer Lipid Membranes (BLM)—RyR1 channels reconstitution was performed as described previously (19). The reconstituted channels exhibiting "low P_o type" gating behavior were the focus of the study. RyR1 is extremely sensitive to Cys oxidation during preparation of SR (19, 27) and results in 60–70% of reconstitutions in BLM yielding channels that exhibit "high P_o type" gating behavior, whereas a small fraction of RyR1 channel reconstituted from these preparations exhibit low P_o type gating behavior (19, 27–29). Low P_o type channels maintain low open probability over a large range of *cis* (cytoplasmic) Ca^{2+}. Because intact muscle possesses a highly reducing environment, the functional consequences of adding Homer proteins to the *cis* chamber focused on reconstituted channels exhibiting low P_o type gating behavior to better reflect the native environment within junctions of intact skeletal muscle (19, 27). Single channel activity was measured at −40 mV (applied *cis* relative to the *trans*) using a patch clamp amplifier (Dagan 3900). The data were filtered at 1 kHz before acquired at 10 kHz by a DigiData 1200A (Axon Inst., Foster City, CA). The data were analyzed using pClamp 6 (Axon) without additional filtering. Average P_o was calculated from ≥1 min of recording.

Macroscopic Ca^{2+} Flux Measurement—Ca^{2+} transport across SR membranes was performed using the absorbance dye antipyrylazo III (30). SR membranes (50 μg/ml) were equilibrated at 37 °C in a transport buffer consisting of 92 mM KCl, 20 mM K-MOPS (pH 7.0), 7.5 mM pyrophosphate, and 250 μM antipyrylazo III. MgATP (1 mM), 10 μg/ml creatine phosphokinase, and 5 mM phosphocreatine were present to regenerate ATP. Ca^{2+} flux was monitored by measuring antipyrylazo III 710–790 nm absorbance at 2–4-s intervals using a diode array spectrophotometer (model 8452A, Hewlett Packard). Pyrophosphate was previously shown to accumulate into SR and support active Ca^{2+} loading without forming precipitates (30); however, the presence of pyrophosphate buffers extravesicular Ca^{2+} 10-fold, so that in its presence the increase in free Ca^{2+} is ~$1/10^{th}$ of the total Ca^{2+} added.

Calcium Imaging of 1B5 Myotubes—The cultured and differentiated 1B5 (RyR null) myotubes were transduced with either wild type or F1777R/F1782R RyR1 amplicons as previously described (21). Within 24–36 h after transduction, the cells were loaded with the calcium indicator dye Fluo-4 at 37 °C, for 30 min in imaging buffer (125 mM NaCl, 5 mM KCl, 2 mM $CaCl_2$, 1.2 mM $MgSO_4$, 6 mM glucose, and 25 mM HEPES, pH 7.4) supplemented with 0.05% bovine serum albumin and 5 μM Fluo-4 (Molecular Probes Inc., Eugene, OR). The cells were washed with imaging buffer before being transferred to a Nikon Diaphot microscope. Fluo-4 was excited at 494 nm using the output of a DeltaRam fluorescence imaging system (Photon Technology International, Princeton, NJ). Fluorescence emission was measured at 516 nm using a 40× quartz objective. Data presented as the 516 nm emissions of Fluo-4 were collected with an intensified CCD camera (Solamere Technology Group) from individual cells. Caffeine- and K^+-evoked Ca^{2+} transients were generated by exposing the cells for 10 s to increasing concentrations of caffeine or KCl. Each test was followed by a 30-s wash allowing the intracellular Ca^{2+} to return to base line. The data were presented as 1) the percentages of myotubes responding to a given stimulus and 2) the normalized magnitude of the transient, $F - F_o/F_o$ (*i.e.* F/F_o), where F_o is the mean base-line fluorescence at rest and F is the peak fluorescence in response to the stimulus. The data were recorded from at least 30 myotubes/treatment.

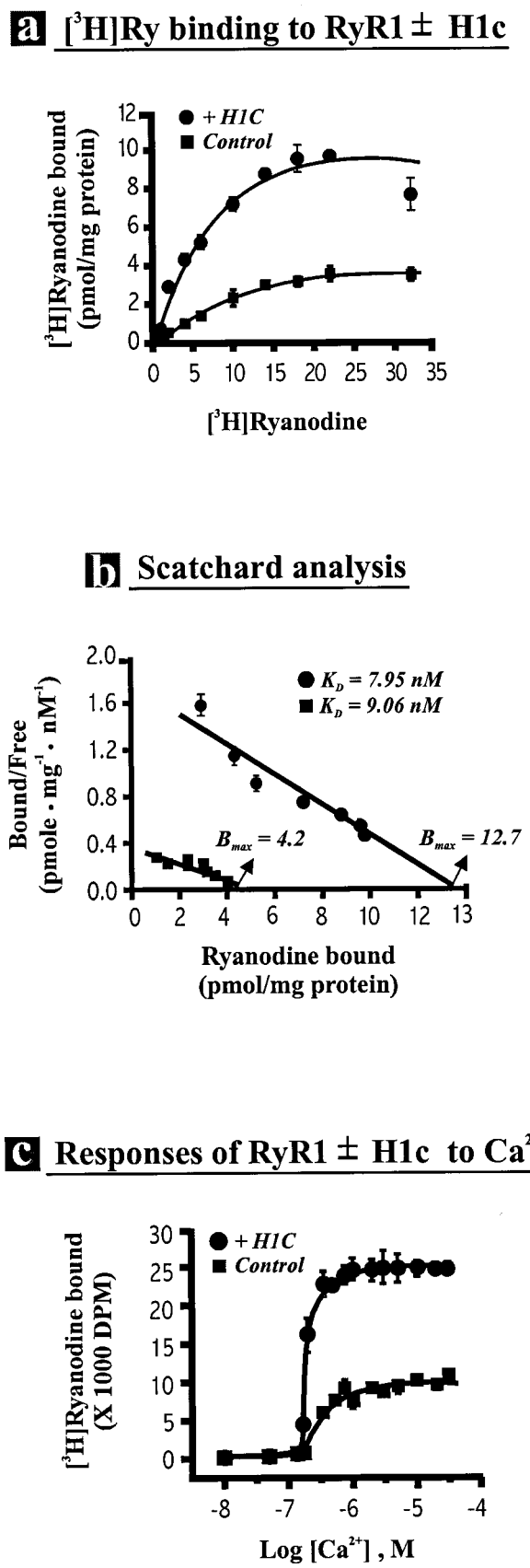

FIG. 3. **Homer increases the maximum density of high affinity [^{3}H]ryanodine binding and amplifies to junctional SR.** *a*, equilibrium binding curves of [^{3}H]ryanodine and 50 μg/ml junctional SR were performed using competition with unlabeled ryanodine (cold titration). The presence of 50 nM GST-H1c (*H1C*) increased occupancy over the entire dose-response curve compared with the GST control. *b*, Scatchard analysis reveals that H1c increases maximum receptor occupancy (B_{max}) 3-fold without altering affinity (K_D) (*a* and *b*; data points are the means ± S.D. from two independent experiments each performed in triplicate). *c*, H1c enhances the efficacy of Ca^{2+} toward activating high affinity [^{3}H]Ry binding 2.5-fold compared with control, without altering the half-activation constant (EC_{50} = 210 *versus* 280 nM, respectively; mean of n = 8). Free Ca^{2+} concentration was adjusted by the addition of $CaCl_2$ and EGTA based on calculations from Bound and Determined software (53).

RESULTS AND DISCUSSION

Homer Proteins Physically Interact with RyR1—An N-terminal EVH1 domain mediates Homer binding to target proteins by contacting specific proline-rich (Homer ligand) sequences found within mGluR1, mGluR5, and the IP_3R (7). Putative Homer ligand sequences are also present in RyR1 (7). Because Homer proteins are expressed in skeletal muscle (2), we examined the possible *in vivo* association of Homer with RyR in immunoprecipitation assays from detergent (1% CHAPS) extracts of rat skeletal muscle. Antibodies for Homer1c (H1c), Homer2, and Homer3 co-precipitated RyR1, whereas the preimmune sera failed to do so (Fig. 1*a*). The interaction of RyR1 with Homer proteins was independently confirmed using GST pull-down assays with GST-Homer1c and GST-Homer3 fusion protein and detergent extracts of skeletal muscle (RyR1) (Fig. 1*b*; lanes GST-H1c and GST-H3). To examine the presence of endogenous Homer proteins in commonly used preparations of junctional SR enriched in RyR1, we isolated several membrane preparations from rabbit skeletal muscle by sucrose density gradient centrifugation and probed them by Western blot analysis with RyR1- and Homer-specific antibodies (Fig. 1*c*). In every junctional SR preparation tested, H1c co-purified with RyR1, although the relative amounts of the H1c varied from preparation to preparation. Homer3 was also co-purified with RyR1 but was not detected in every junctional SR preparation examined (Fig. 1*c*). In all four preparations that were analyzed, H1c and Homer3 proteins were less enriched than RyR1. Because Homer is a cytosolic protein, these results are consistent with the physical association of Homer with RyR1 and indicate that the co-enrichment of Homer relative to RyR1 varies from preparation to preparation. Presumably, Homer proteins variably dissociated from the RyR1 complex during purification of junctional SR membranes.

H1C and H1-EVH1 Enhance RyR1 Gating—To examine the functional consequence of the protein-protein interaction, we determined whether Homer could modify RyR1 channel gating behavior using the BLM method. Single RyR1 channels were reconstituted with an artificial BLM by inducing fusion of purified junctional SR vesicles. Those channels exhibiting the low P_o gating mode (19, 27–29) were selected for examining the influence of exogenous Homer protein added to the cytoplasmic (*cis*) side of the channel measured under voltage clamp conditions. Both the long form H1c (Fig. 2*a*) and short form H1-EVH1 lacking the coiled-coil domain (Fig. 2*b*) were highly potent and efficacious toward enhancing RyR1 channel open probability (P_o). With 5 nM H1c added to the *cis* chamber, P_o increased ~10-fold. H1-EVH1 was equally effective but 7-fold less potent (34 nM H1-EVH1 needed to enhance P_o ~10-fold). The murine homolog of Ena (Mena) possesses an EVH1 domain that is structurally similar to Homer but binds a distinct proline-rich sequence (7). Mena lacked detectable activity on channel P_o at the highest concentration tested (50 nM). Both H1-EVH1 and H1c shortened channel closed dwell time by over 100-fold without significantly altering open dwell time (data not shown). We also examined the effects of the immediate-early gene product Homer1a-EVH1 on high P_o gating mode channels reconstituted in BLM. Homer1a-EVH1 (40 nM) signif-

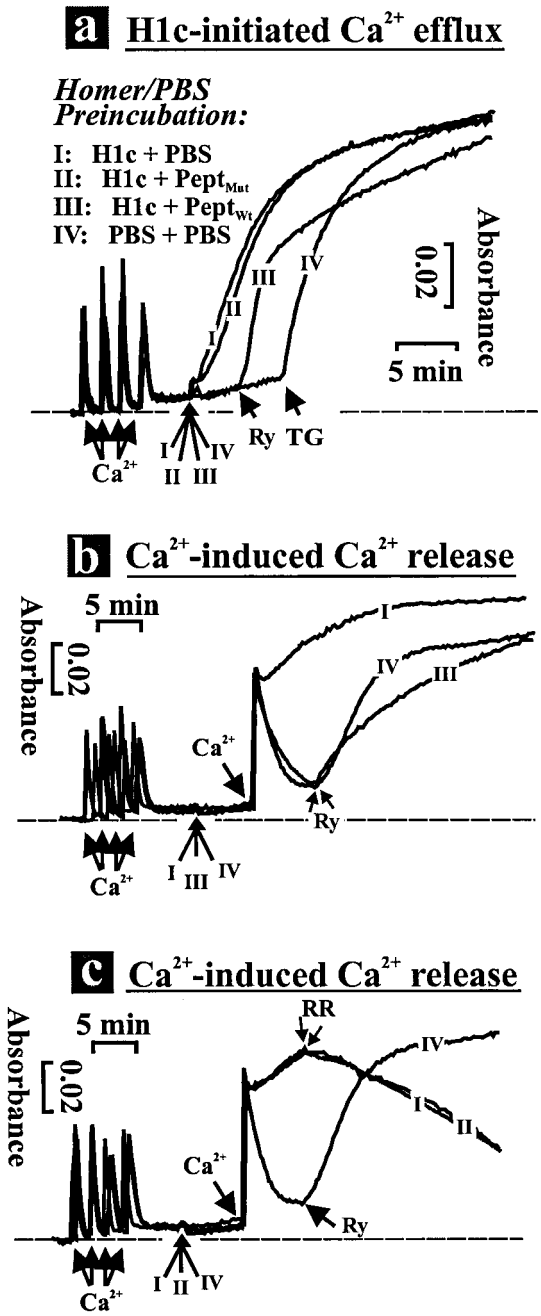

FIG. 4. **Enhancement of RyR1 channel function by Homer is specifically blocked by competing peptide.** H1c was preincubated with 1000× synthetic wild type Homer-binding peptide ($Pept_{wt}$), synthetic peptide missing the critical phenylalanine ($Pept_{mut}$), or PBS at 37 °C for 10 min. After completion of preloading of SR with 160 μM Ca^{2+}, Homer in the presence or absence of $Pept_{wt}$ or $Pept_{mut}$ was introduced. The final concentration of the H1c in the transport buffer was 20 nM (*a*) or 8 nM (*b* and *c*). 10 μM ryanodine (Ry) or Ruthenium Red (RR) was added to activate or inhibit RyR1, whereas 0.5 μM thapsigargin (*TG*) was introduced to inhibit SR Ca^{2+} pumps. In *b* and *c*, the final concentration of Ca^{2+} used to induce Ca^{2+} release was 60 μM. Summary data represent the mean of 21 (*a*), 6 (*b*), or 6 (*c*) repetitions of these experiments.

icantly enhanced the gating activity of in the presence of 7 μM *cis* Ca^{2+} (~4-fold; not shown).

Mechanism of Homer Modulation of RyR1—The manner in which Homer proteins enhances RyR1 activity was examined in more detail by measuring their influence on the binding of [^{3}H]ryanodine to skeletal muscle JSR. Because [^{3}H]ryanodine binds with high affinity to an open state of the RyR channel, occupancy of [^{3}H]ryanodine-binding sites provides a convenient biochemical indicator of modulation of the open probability of the channel by exogenously added ligands (24–26). When GST was included in the binding medium, occupancy of [^{3}H]ryanodine was indistinguishable from control (Fig. 2*c*). Similarly, [^{3}H]ryanodine binding was unaltered by inclusion of Mena (≤100 nM). In marked contrast, 50 nM H1c or its fusion protein, GST-H1c, enhanced the binding of 5 nM [^{3}H]ryanodine by nearly 5-fold (Fig. 2*c*). The actions of GST-H1c measured in the presence [^{3}H]ryanodine at a concentration well below its K_D (0.5 nM) resulted in ~8-fold enhancement of occupancy (Fig. 2*c*, *right panel*) consistent with the effects of Homer protein on enhancing channel P_o in BLM studies (Fig. 2*a*). At a concentration of 5 nM [^{3}H]ryanodine, the addition of 50 nM H1-EVH1 mimicked the activity of full-length H1c but exhibited smaller (<2-fold) but statistically significant ($p < 0.05$) enhancement in binding compared with control. When tested at subsaturating [^{3}H]ryanodine (0.5 nM), the addition of 150 nM H1-EVH1 increased binding ~5-fold, whereas 50 nM H1c increased binding ~8-fold (Fig. 2*c*). This demonstrates that both forms have a similar ability to enhance RyR1 activity consistent with their ability to enhance the P_o of channels reconstituted in BLM (Fig. 2*b*). The 3-fold difference in the potency observed with the long and short forms of Homer on RyR1 could be attributed to the multivalency of H1c that may optimize conformational interaction with RyR1 oligomeric units. As a further control, we found that the W24A point mutant of H1-EVH1, which does not bind Homer ligands (7), had negligible activity on altering the binding of [^{3}H]ryanodine to RyR1 under the stated assay condition (Fig. 2*c*). These results support the hypothesis that specific protein-protein interactions between Homer proteins and RyR1 can variably enhance the gain of signaling events mediated through Ca^{2+}-induced Ca^{2+} release (CICR), and hence Ca^{2+} released from SR, by influencing the fraction of RyR channels within junctional SR responsive to physiological activators.

To further test the hypothesis, [^{3}H]ryanodine-binding curves were performed in the presence of nearly optimal Ca^{2+} for channel activation (1 μM) and in the absence or presence of Homer protein (Fig. 3*a*). Scatchard analysis revealed that H1c enhanced the binding of [^{3}H]ryanodine over the complete range of concentrations, enhancing maximum occupancy 3-fold (from B_{max} = 4.2 and 12.7 pmol mg^{-1} in the absence and presence of 50 nM H1c, respectively) without significantly altering binding affinity (K_D = 7.95 and 9.06 nM, respectively; Fig. 3*b*). These results indicate that formation of H1c-RyR1 complexes *in vitro* significantly increased the density of Ca^{2+}-responsive channels within the SR membrane. Because Homer protein appears to dissociate from SR preparations during biochemical enrichment of RyR1, the ability of exogenous Homer to increase the density of functional RyR1 able to bind ryanodine in a Ca^{2+}-dependent manner likely results from formation of new protein-protein complexes that may have been lost during preparation of junctional SR membranes.

Although in skeletal muscle CICR is not necessary to initiate E-C coupling, nor is it necessary to engage retrograde signaling (32), it is generally agreed that Ca^{2+} is an important physiological modulator of RyR1 in skeletal muscle. Several ligands have been shown to influence the sensitivity of RyR to activation by Ca^{2+} (24, 26). Using [^{3}H]ryanodine binding analysis near K_D for the radioligand, H1c (50 nM) did not significantly shift the sensitivity of RyR1 to activation by Ca^{2+} relative to control (EC_{50} = 210 *versus* 280 nM Ca^{2+}, respectively; Fig. 3*c*). However, H1c did enhance maximal occupancy 2.5-fold, indicating an enhanced "gain" of RyR1 toward activation by Ca^{2+} consistent with an increase in the density of Ca^{2+}-responsive RyR1 complexes.

Homer Enhances CICR and Caffeine—A functional corre-

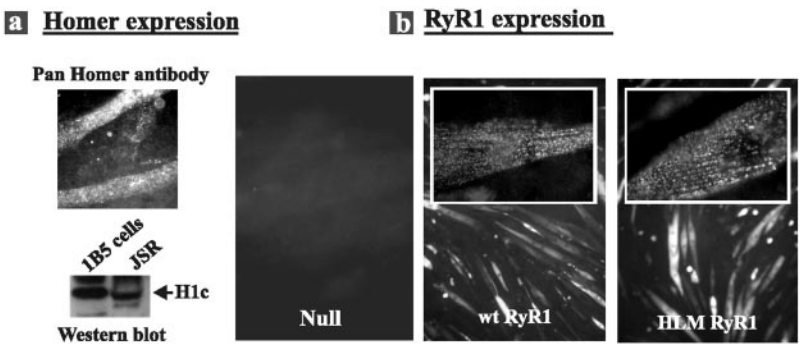

FIG. 5. **Expression of RyR1 possessing a mutation of a putative Homer-ligand sequence in 1B5 myotubes.** *a* shows that 1B5 myotubes constitutively express immunoreactive Homer protein. The *upper panel* shows 1B5 cells expressing *wt* RyR1 immunostained with pan Homer antibody as described under "Materials and Methods" at 10× magnification. The same results were observed with 1B5 myotubes expressing RyR1 possessing point mutation F1777R/F1782R. The *lower panel* shows results from Western analysis of the whole membrane fraction obtained from 1B5 myotubes and rabbit skeletal muscle junctional SR probed with Homer1c-selective antibody. *b*, immunocytochemical analysis of 1B5 myotubes at 10× before (*left panel*) and after transduction with HSV-1 virions containing wild type (*wt*) RyR1 (*middle panel*) and full-length RyR1 containing a point mutation within the putative Homer ligand domain (HLM, *right panel*). 100× magnification inserts in the *middle* and *right panels* show that both wild type and HLM RyR1 have the characteristic punctate staining pattern of RyR1 when it is targeted properly to peripheral junctions.

late to the results obtained from radioligand receptor binding analysis was undertaken to understand how H1c influences macroscopic Ca^{2+} efflux elicited by either Ca^{2+} (CICR) or caffeine from actively loaded skeletal muscle SR vesicles (Fig. 4, *b* and *c*). This assay utilizes pyrophosphate to support active loading of Ca^{2+} into the vesicles (30). After calcium loading, the addition of H1c to a subthreshold concentration (8 nM) that did not directly initiate net Ca^{2+} efflux from the SR vesicles enhanced the initial rate of RyR1-mediated Ca^{2+} elicited by subsequent addition of either optimal 80 μM total Ca^{2+} (8.0 μM free Ca^{2+}) or saturating caffeine (10 mM) 7.9- and 8.2-fold, respectively. Thus, H1c enhanced the maximum efficacy of both Ca^{2+} and caffeine for activation of RyR1.

Homer Modulation of RyR1 Is Blocked by Specific Peptide—The specificity of H1c for enhancing Ca^{2+} release from SR was examined by preincubating H1c with a synthetic "blocking" peptide that mimics the Homer ligand within the C terminus of mGluR-1 (1). Fig. 4*a* (*trace I*) demonstrates that addition of saturating (20 nM) H1c induced net Ca^{2+} release from actively loaded SR vesicles. In the absence of added Homer, Ca^{2+} was not released until the addition of either ryanodine (10 μM; *trace III*) or the SR Ca^{2+} pump inhibitor thapsigargin (0.5 μM; *trace IV*). The effect of H1c could be blocked by the addition of 50 μM wild type peptide ($Pept_{wt}$) but not by a point mutant of the blocking peptide ($Pept_{mut}$) that lacks Homer binding activity (1) (Fig. 4*a*, trace II). $Pept_{wt}$ does not block release by subsequent addition of ryanodine. $Pept_{wt}$, but not $Pept_{mut}$, also prevented the ability of H1c to amplify CICR after active loading of 160 μM Ca^{2+} into SR (Fig. 4, *b* and *c*). CICR induced by the addition of 60 μM Ca^{2+} in the presence of 8 nM H1c exhibited indistinguishable rates of Ca^{2+} release in the presence or absence of $Pept_{mut}$ (Fig. 4*c*, *traces I* and *II*). Subsequent addition of Ruthenium Red (10 μM), an RyR channel blocker, resulted in active re-uptake of Ca^{2+} into SR vesicles. However, in the presence of $Pept_{wt}$ (Fig. 4*b*, *trace III*), the addition of 60 μM Ca^{2+} displayed a net Ca^{2+} uptake into SR because SR Ca^{2+} pump-transport into the vesicles surpassed the amount of release through RyR1. Active accumulation could be interrupted abruptly and was quickly followed by Ca^{2+} release after subsequent addition of 10 μM ryanodine (Fig. 4, *b* and *c*, *trace IV*). As further evidence of its specificity, we confirmed that $Pept_{wt}$ did not affect modulation of RyR1 by the scorpion toxin maurocalcine, a potent activator of RyR1 (31) (not shown).

Taken together, these results revealed that physical association of H1c with RyR1 dramatically enhanced Ca^{2+} responsiveness of RyR1 at the level of the single channel and underlies the increased "gain" of RyR1-mediated Ca^{2+} efflux units within junctional SR (defined by two independent measures, macroscopic Ca^{2+} efflux (CICR) and [^{3}H]ryanodine binding density). These actions of Homer protein exhibited a high degree of molecular specificity and were mediated by their unique EVH1 domain.

RyR1 Homer-binding Domain Regulates Gain—Conformational changes in IP_3R caused by IP_3 binding and store depletion was shown to provide a retrograde signal to opening of store-operated Ca^{2+} channels in the plasma membrane (33, 34), similar to the bi-directional signaling between RyR1 and α_{1S}-DHPR in skeletal muscle that is essential for engaging E-C coupling (17). Moreover, evidence for conformational coupling between RyR and store-operated Ca^{2+} channels has been recently presented (35, 36). Thus, conformational coupling appears to be a fundamental mechanism involved in generating localized Ca^{2+} signals. Both RyR and α_{1S}-DHPR possess discrete polyproline sequences that are putative Homer ligands. RyR1 contains a putative Homer-ligand domain between amino acids 1773 and 1783. A second putative Homer binding domain can be found in RyR1 (PPPGYA; amino acids 804–809), where the essential hydrophobic phenylalanine is substituted with tyrosine.

We therefore tested the hypothesis that Homer is involved in modulating the strength of depolarized-induced Ca^{2+} release in intact cells. 1B5 dyspedic skeletal myotubes express all the proteins known to be associated with the mature triadic junction but lack expression of the three RyR isoforms (23, 37). Transduction of 1B5 myotubes with wild type RyR1 cDNA reconstituted bi-directional signaling between RyR1 and α_{1S}-DHPR and directed the organization of α_{1S}-DHPR particles into organized arrays of tetrads (38, 39). Homer1 protein was detected in 1B5 myotubes by immunocytochemical and Western blot analyses (Fig. 5*a*).

The possible functional role of one of the putative Homer-binding sites of RyR1 was tested by incorporating site-directed mutations (F1777R/F1782R) within the full-length protomer. The substitutions were chosen based on the recent data showing that hydrophobic phenylalanine C-terminal to polyprolines are essential for Homer binding (7). RyR protomers from 1B5 myotubes expressing full-length wild type and F1777R/F1782R RyR1 proteins exhibited the same mobility by SDS-PAGE (not shown) and show similar levels of expression by immunocytochemistry. At higher magnification both *wt* and F1777R/F1782R RyR1 exhibited the characteristic punctate pattern of

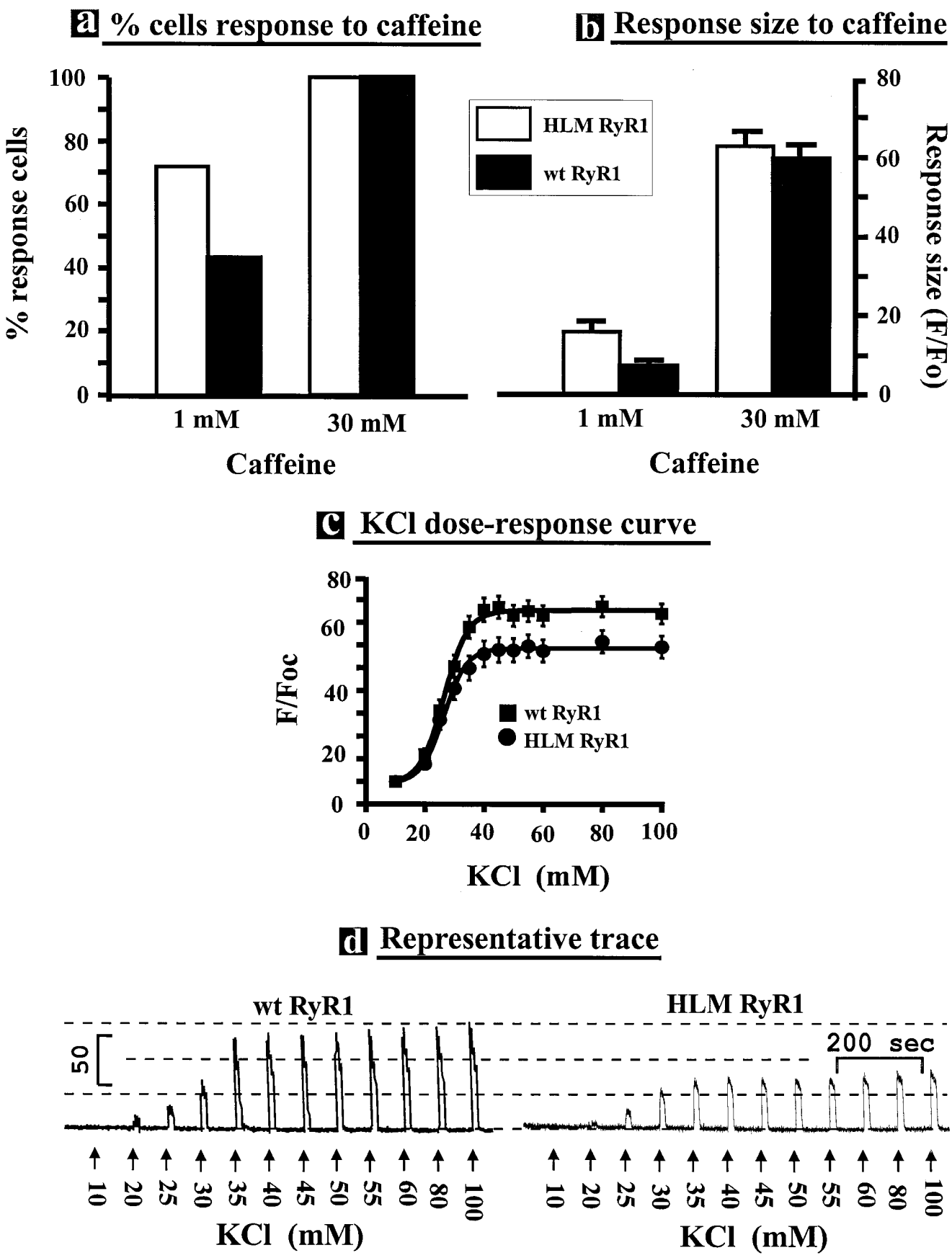

FIG. 6. **Mutation of a putative Homer-ligand sequence of RyR1 attenuates excitation-contraction coupling in 1B5 myotubes.** *a* shows the responses of 1B5 myotubes expressing wild type and the putative HLM (F1777R/F1782R RyR1) to threshold (1 mM) and saturating (30 mM) caffeine. 40% fewer myotubes responded to the threshold concentration of caffeine, whereas all myotubes responded to saturating caffeine. The normalized amplitude of responses to threshold caffeine were 56% smaller ($p < 0.001$) in HLM *versus* wild type but were not different at saturating caffeine. The data were analyzed from 68 and 92 wild type and HLM myotubes, respectively. *c* and *d* show the K^+-evoked Ca^{2+} transients following

expression within the myotubes, which has previously been shown to be consistent with targeting of RyR protein to peripheral junctions (Fig. 5*b*) (38, 39).

Both wild type and the putative Homer ligand mutation (HLM; F1777R/F1782R) RyR1 responded to caffeine challenges. However, the percentage of HLM myotubes responding to a threshold concentration of caffeine (1 mM) was 39.6% lower than wild type myotubes (43.5% *versus* 72.0% of $n = 92$ and 68 myotubes, respectively; Fig. 6*a*, *left bars*). When challenged with saturating caffeine (30 mM), the frequency of responses with HLM and wild type myotubes were both 100%. The normalized magnitude of the Fluo-4 fluorescence signal (F/F_o) is a quantitative measure of the amount of Ca^{2+} mobilized in response to direct activation of release channels by caffeine. The magnitude of the responses to 1 mM caffeine was 56.6% smaller ($F/F_o = 6.8\%$ *versus* 15.7%; $p = 0.003$) in myotubes expressing HLM. However, 30 mM caffeine elicited Ca^{2+} responses whose magnitude were indistinguishable between wild type and HLM myotubes, indicating that the SR stores of both cell types were filled with Ca^{2+} to similar levels (Fig. 6*a*, *right bars*).

Expression of either wild type or HLM cDNAs in 1B5 myotubes also restored Ca^{2+} responses to K^+ depolarization consistent with restoration of skeletal type excitation-contraction coupling, and the amplitude of this response increased in a saturable manner with increasing K^+ concentration between 10 and 100 mM (Fig. 6, *c* and *d*). The expressed proteins produced Ca^{2+} transients that were kinetically identical, and the apparent potency for producing K^+-evoked Ca^{2+} transients was unaltered by the mutation ($EC_{50} = 26.6 + 1.2$ and $27.0 + 1.2$ mM for wild type and mutant protein, respectively). Importantly, however, the maximum amplitude of the K^+-evoked Ca^{2+} transients produced by cells expressing HLM were 33% smaller than those produced by wild type RyR1 (mean $F/F_o = 76 + 0.85$ and $58 + 2.0$; $n = 34$ and 48 cells for wild type and HLM, respectively; $p < 0.001$), demonstrating Homer's importance in modulating depolarization induced Ca^{2+} release. The possible existence of a second Homer ligand domain within RyR1 (amino acids 804–809) and its functional role remains to be investigated.

Functional Significance of Interactions between RyR1 and Homer Proteins—The present study demonstrates that Homer binding directly enhances responses of RyR1 to physiological and pharmacological stimuli. This activity is conferred by the EVH1 domain and does not require the cross-linking adapter function of Homer. However, multimeric H1c does appear to significantly enhance the potency toward enhancing RyR1 responses. Homer is the first example of an "adapter" that also modifies signaling properties of its target protein. Multi-PDZ domain proteins are reported to activate ion channels, but this activity is mediated by simple physical cross-linking (14). The nanomolar affinities required for channel modulation with full-length RyR and the complete long and short forms of Homer indicate a structurally specific interaction. Previous studies that used peptides to block the binding of EVH domains with their target proteins suggested affinities in the micromolar range (1, 8). Because our studies used full-length proteins, it is inferred that additional structure is important for optimizing these binding interactions. Thus, RyR1 that is bound by constitutively expressed full-length Homer could reinforce its known adapter role, resulting in signaling microdomains that are uniquely primed for Ca^{2+} signals.

The present findings reveal that Homer proteins through their direct interaction with RyR1 can modulate the gain of E-C coupling. This can occur in three ways. First, the interaction of constitutively expressed H1c could bind to one to four channel protomers to regulate cooperativity associated with channel activation. Second, H1c multimers could cross-link multiple RyR1 oligomers to facilitate coupled gating among channels elicited by FKBP12 (40). Because localized Ca^{2+} sparks occur upon release of Ca^{2+} through a cluster of RyR (41), it is interesting to note that H1c has been recently shown to induce sparks in frog skeletal muscle (42). Homer-RyR associations may therefore be a significant physiological regulator of spark activity that contributes to Ca^{2+} waves that sweep through cells and subsequently activate myocyte contraction. Third, multimeric H1c could directly cross-link RyR1 with α_{1S}-DHPR to enhance the efficiency of E-C coupling in a manner already described for mGluR1 and IP_3R (1, 7). Whether Homer interactions with a putative binding site on α_{1S}-DHPR contribute to modulation of E-C coupling remains to be determined.

Homer short form (*i.e.* H1a-EVH1) is encoded by a prematurely terminated transcript that lacks the coiled-coil domain that is required for the formation of Homer multimers. The currently favored mechanism for how Homer proteins regulate signaling functions suggests that the H1-EVH1, an immediate-early gene product, is rapidly expressed in response to cellular activity, whereas long form H1c is constitutively expressed. In this scheme, H1c plays an adapter function, linking target proteins such as mGluR1 and IP_3R in neurons. Immediate-early expression of H1-EVH1 acts in a dominate-negative fashion by competing with existing H1c complexes, thereby impairing the formation and maintenance of Homer-mediated cluster of protein complexes (2). However, experimental evidence for a more dynamic role for Homer proteins in cellular regulation has recently been defined (13, 43–45). For example, experiments using single particle tracking demonstrated that the composition of Homer-mediated clustering of protein complexes is highly dynamic. The exchange of the proteins between dispersed and clustered states is fast and is regulated during physiological processes (44, 45). The present results suggest that the catalytic activity of Homer proteins toward RyR may provide one mechanism linking Ca^{2+} signals with dynamic regulation of Homer-mediated protein clustering.

One anticipated consequence of Homer catalytic activity is to increase the spatial fidelity of signaling beyond what can be achieved by simple physical coupling. Homer and RyR proteins are widely expressed, and it may be anticipated that their physical and functional interactions identified here contribute to temporal and spatial patterning of intracellular Ca^{2+} signaling. In skeletal muscle, release of Ca^{2+} through RyR1 is the key event linking membrane depolarization and mechanical activity during E-C coupling. In neurons, Homer proteins play a special role in adaptation to cellular activity. CICR has been demonstrated in a number of neuronal cell types (46–48). Evidence for the role of RyR in the regulation of specific aspects of neuronal plasticity, dendritic growth, and spatial learning has recently been demonstrated (49–52). The present results predict that RyR1-Homer interactions may also contribute elements of structural and functional regulation important for synaptic plasticity that are likely to direct signal processing and shape neuronal circuits.

10 s of varied K^+ challenge on dyspedic 1B5 myotubes transduced with either wild type or HLM cDNA. Ca^{2+} transients were independent of extracellular Ca^{2+} entry and represent skeletal type excitation-contraction coupling. Although the K^+ concentration producing half-maximal amplitude was not different (26.1 *versus* 26.7 mM), the maximal amplitude of the transients was 33% smaller ($p < 0.001$) for RyR1 lacking the critical phenylalanines within a putative Homer ligand domain. The measurements are the means from 34 and 47 individual cells for wild type and HLM.

REFERENCES

1. Tu, J. C., Xiao, B., Yuan, J, P., Lanahan, A. A., Leoffert, K., Li, M., Linden, D. J., and Worley, P. F. (1998) *Neuron* **21,** 717–726
2. Xiao, B., Tu, J. C., and Worley, P. F. (2000) *Curr. Opin. Neurobiol.* **10,** 370–374
3. Brakeman, P. R., Lanahan, A. A., OBrien, R., Roche, K., Barnes, C. A., Huganir, R. L., and Worley, P. F. (1997). *Nature*, **386,** 284–288
4. Soloviev, M. M., Ciruela, F., Chan, W. Y., and McIlhinney, R. A. J. (2000) *Eur. J. Biochem.*, **267,** 634–639
5. Sandona, D.; Tibaldo, E., and Volpe, P. (2000) *Biochem. Biophys. Res. Commun.* **279,** 348–353
6. Gertler, F. B., Niebuhr, K., Reinhard, M., Wehland, J., and Soriano, P. (1996) *Cell* **87,** 227–239
7. Beneken, J., Tu, J. C., Xiao, B., Nuriya, M., Yuan, J. P., Worley, P. F., and Leahy, D. J. (2000) *Neuron* **26,** 143–154
8. Tu, J. C., Xiao, B., Naisbitt, S., Yuan, J. P., Petralia, R. S., Brakeman, P., Doan, A., Aakalu, V. K., Lanahan, A. A., Sheng, M., and Worley, P. F. (1999) *Neuron* **23,** 583–592
9. Naisbitt. S, Kim. E., Tu, J. C., Xiao, B., Sala, C., Valtschanoff, J., Weinberg, R. J., Worley, P. F., and Sheng, M. (1999) *Neuron* **23,** 569–582
10. Kato, A., Ozawa, F., Saitoh, Y., Fukazawa, Y., Sugiyama, H., and Inokuchi, K. (1998) *J. Biol. Chem.* **273,** 23969–23975
11. Sun, J., Tadokoro, S., Imanaka, T., Murakami, S. D., Nakamura, M., Kashiwada, K., Ko, J., Nishida, W., and Sobue, K. (1998) *FEBS Lett.* **437,** 304–308
12. Xiao, B., Tu, J. C., Petralia, R. S., Yuan, J. P., Doan, A., Breder, C. D., Ruggiero, A., Lanahan, A. A., Wenthold, R. J., and Worley, P. F. (1998) *Neuron* **21,** 707–716
13. Tadokoro, S., Tachibana, T., Imanaka, T., Nishida, W., and Sobue, K. (1999) *Proc. Natl. Acad. Sci. U. S. A.* **96,** 13801–13806
14. Wang, S., Yue, H., Derin, R. B., Guggino, W. B., and Li, M. (2000) *Cell* **103,** 169–179
15. Ango, F., Prezeau, L., Muller, T., Tu, J. C., Xiao, B., Worley, P. F., Pin, J. P., Bockaert, J., and Fagni, L. (2001) *Nature* **411,** 962–965
16. Franzini-Armstrong, C., Protasi, F., and Ramesh, V. (1998) *Ann. N. Y. Acad. Sci.* **853,** 20–30
17. Nakai, J., Dirksen, R. T., Nguyen, H. T., Pessah, I. N., Beam, K. G., and Allen, P. D. (1999) *Nature* **380,** 72–75
18. Saito, A., Seiler, S., Chu, A., and Fleischer, S. (1984) *J. Cell Biol.* **99,** 875–885
19. Feng, W., Liu, G., Allen, P. D., and Pessah, I. N. (2000) *J. Biol. Chem.* **275,** 35902–35907
20. Deleted in proof
21. Wang, Y., Fraefel, C., Protasi, F., Moore, R. A., Fessenden, J. D., Pessah, I. N., DiFrancesco, A., Breakefield, X., and Allen, P. D. (2000) *Am. J. Physiol.* **278,** C619–C626
22. Ivanenko, A., Baring, M. D., Airey, J. A., Sutko, J. L., and Kenyon, J. L. (1993) *J. Neurophysiol.* **70,** 710–722
23. Moore, R. A., Nguyen, H., Galceran, J., Pessah, I. N., and Allen, P. D. (1998) *J. Cell Biol.* **140,** 843–851
24. Pessah, I. N., Waterhouse, A. L., and Casida, J. E. (1985) *Biocem. Biophys. Res. Commun.* **128,** 449–456
25. Pessah, I. N., Francini, A. O., Scales, D. J., Waterhouse, A. L., and Casida, J. E. (1986) *J. Biol. Chem.* **261,** 8643–8648
26. Pessah I. N, Stambuk, R. A., and Casida, J. E. (1987) *Mol. Pharmacol.* **31,** 232–238
27. Sun, J. H, Xin, C. L., Eu, J. P, Stamler, J. S., and Meissner, G. (2001) *Proc. Nat. Acad. Sci. U. S. A.* **98,** 11158–11162
28. Marengo, J. J., Hidalgo, C., and Bull, R. (1998) *Biophys. J.* **74,** 1263–1277
29. Murayama, T., Oba, T., Katayama, E., Oyamada, H., Oguchi, K., Kobayashi, M., Otsuka, K., and Ogawa, Y. *J. Biol. Chem.* **274,** 17297–17308
30. Palade, P. (1987) *J. Biol. Chem.* **262,** 6135–6141
31. Fajloun, Z., Kharrat, R., Chen, L., Lecomte, C., di Luccio, E., Bichet, D., Rochat, H., Allen, P. D., Pessah, I. N., DeWaard, M., and Sabatier, J. M. (2000) *FEBS Lett.* **469,** 179–185
32. O'Brien, J. J., Feng, W., Allen, P. D., Chen, S. R. W., Pessah, I. N., and Beam, K. G. (2002) *Biophys. J.* **82,** 2428–2435
33. Kiselyov, K., Xu, X., Mozhayeva, G., Kuo, T., Pessah, I., Mignery, G., Zhu, Z., Birnbaumer, L., and Muallem, S. (1998) *Nature* **396,** 478–482
34. Li, H. S., Xu, X. Z., and Montell, C. (1999) *Neuron* **24,** 261–273
35. Kiselyov, K., Shin, D. M., Wang, Y., Pessah, I. N., Allen, P. D., and Muallem, S. (2000) *Mol. Cell* **6,** 421–431
36. Kurebayashi, N., and Ogawa, Y. (2001) *J. Physiol.* (*Lond.*) **533,** 185–199
37. Fessenden, J. D., Wang, Y., Moore, R. A., Chen, S. R. W., Allen, P. D., and Pessah, I. N. (2000) *Biophys. J.* **79,** 2509–2525
38. Protasi, F., FranziniArmstrong, C., and Allen, P. D. (1998) *J. Cell Biol.* **140,** 831–842
39. Protasi, F., Takekura, H., Wang, Y. M., Chen, S. R. W., Meissner, G., Allen, P. D., and Franzini-Armstrong, C. (2000) *Biophys. J.* **79,** 2494–2508
40. Marx, S. O., Ondrias, K., and Marks, A. R. (1998) *Science* **281,** 818–821
41. Gonzalez, A., Kirsch, W. G., Shirokova, N., Pizarro, G., Grum, G., Pessah, I. N., Stern, M. D., Cheng, H., and Rios, E. (2000) *Proc. Natl. Acad. Sci. U. S. A.* **97,** 4380–4385
42. Ward, C. W., Tu, J. C., Worley, P. F., and Schneider, M. F. (2002) *Biophys. J.* **82,** 284 (abstr.)
43. Thomas, U. (2002) *J. Neurochem.* **81,** 407–413
44. Serge, A., Fourgeaud, L., Hemar, A., and Choquet, D. (2002) *J. Neurosci.* **22,** 3910–3920
45. Okabe, S., Urushido, T., Konno, D., Okado, H., and Sobue, K. (2001) *J. Neurosci.* **21,** 9561–9571
46. Llano, I., DiPolo, R., and Marty, A. (1994) *Neuron* **12,** 663–673
47. Kano, M., Garaschuk, O., Verkhratsky, A., and Konnerth, A. (1995) *J. Physiol.* **487,** 1–16
48. Usachev, Y. M., and Thayer, S. A. (1997) *J. Neurosci.* **17,** 7404–7414
49. Korkotian, E., and Segal, M. (1999) *Proc. Natl. Acad. Sci. U. S. A.* **96,** 12068–12072
50. Sun, M. K., Nelson, T. J., and Alkon, D. L. (2000). *Proc. Natl. Acad. Sci. U. S. A.* **97,** 12300–12305
51. Alkon, D. L., Nelson, T. J., Zhao, W. Q., and Cavallaro, S. (1998) *Trends Neurosci.* **21,** 529–537
52. Futatsugi, A., Kato, K., Ogura, H., Li, S. T., Nagata, E., Kuwajima, G., Tanaka, K., Itohara, S., and Mikoshiba, K. (1999) *Neuron* **24,** 701–731
53. Brooks, S. P., and Storey, K. B. (1992) *Anal. Biochem.* **201,** 119–126